

# Membrane Partitioning of the Cleavage Peptide in Flock House Virus

Dennis T. Bong, Andreas Janshoff, Claudia Steinem, and M. Reza Ghadiri

Departments of Chemistry and Molecular Biology and the Skaggs Institute for Chemical Biology, The Scripps Research Institute, La Jolla, California 92037 USA

**ABSTRACT** Membrane translocation of the ssRNA genome of nodaviruses has been proposed to be mediated by direct lipid-protein interactions between a postassembly autocatalytic cleavage product from the capsomere and the target membrane. We have recently shown that the 21-residue Met→Nle variant of the N-terminal helical domain (denoted  $\gamma_1$ ) of the cleavage peptide in flock house nodavirus increases membrane permeability to hydrophilic solutes and can alter both membrane structure and function, suggesting the possibility of peptide-triggered disruption of the endosomal membrane as a prelude to viral uncoating in the host cytoplasm. Elucidation of partitioning energetics would allow an assessment of the likelihood of this mechanism. We report herein complete thermodynamic characterization of the partitioning of  $\gamma_1$  to phospholipids by lipid-peptide titrations following changes in ellipticity, fluorescence signature, or calorimetric response. These experiments revealed a partitioning energy comparable to natural membrane-active peptide toxins, suggesting that the proposed mechanism may be possible. Additionally, a novel switch in the balance of partitioning forces was found: when the lipid headgroup was changed from zwitterionic to negatively charged, membrane association of the peptide became completely entropy-driven.

## INTRODUCTION

Nodaviruses are nonenveloped RNA animal viruses comprised of a bipartite single-stranded RNA genome encoding three genes packaged within an icosahedral assembly of identical gene products. It is thought that nodaviruses enter cells in a manner analogous to picornaviruses, using receptor-binding-induced endocytosis followed by uncoating concomitant with transmembrane passage of RNA. Interestingly, the infectivity of assembled virions is contingent upon a maturation event common to all nodaviruses in which the particle autocatalytically cleaves a peptide sequence from the C-terminus of the capsid protein (Schneemann et al., 1992; Zlotnick et al., 1994). The connection between infectivity and cleavage is as yet unclear, although structural investigation of nodaviruses (Hosur et al., 1987; Cheng et al., 1994) and other simple RNA viruses (Munshi et al., 1996) has led to the hypothesis (Fisher and Johnson, 1993) that the cleaved sequence plays a key role in effecting transmembrane passage of viral genomic material. Indeed, it has been demonstrated (Schneemann and Marshall, 1998) in flock house nodavirus (FHV) that recognition processes between the C-terminal region of its 44-residue cleavage peptide (called the  $\gamma$ -peptide) and RNA drive packaging specificity. Furthermore, recent studies have shown that the N-terminal region of the  $\gamma$ -peptide can dramatically alter membrane structure (Janshoff et al., 1999) and increase bilayer permeability (Bong et al., 1999). It is therefore possible that these cleavage sequences both guide genome

packaging and interact directly with the endosomal membrane to disrupt the lipid packing and mediate the translocation of the viral genome.

We present a full thermodynamic characterization of the membrane partitioning of the 21-residue Met→Nle variant of the N-terminal helical domain of the  $\gamma$ -peptide from FHV, denoted here as  $\gamma_1$  (Scheme 1). Calorimetry, circular dichroism (CD) and fluorescence spectroscopy allowed us to clearly delineate the energetics of peptide-lipid binding. The presence of negatively charged lipids in biomembranes led us to carry out our measurements on both zwitterionic and negatively charged phospholipids so as to understand the influence of electrostatics on peptide insertion. These data revealed that the membrane-binding energy of this nodaviral peptide is comparable to those of natural membrane-disruptive toxins and antibacterials. The observation of such significant membrane affinity in  $\gamma_1$  is provocative because such high membrane-binding avidity typically accompanies a membrane binding *function*. When the bilayer partitioning ability of  $\gamma_1$  is coupled to its location in the viral capsid, its proposed role in transmembrane passage of viral material seems much more possible. Although the function of the  $\gamma_1$  region in the viral lifecycle remains speculative, these data strengthen the hypothesis of cleavage peptide-mediated transmembrane passage of RNA in nodaviruses.

## MATERIALS AND METHODS

### Materials

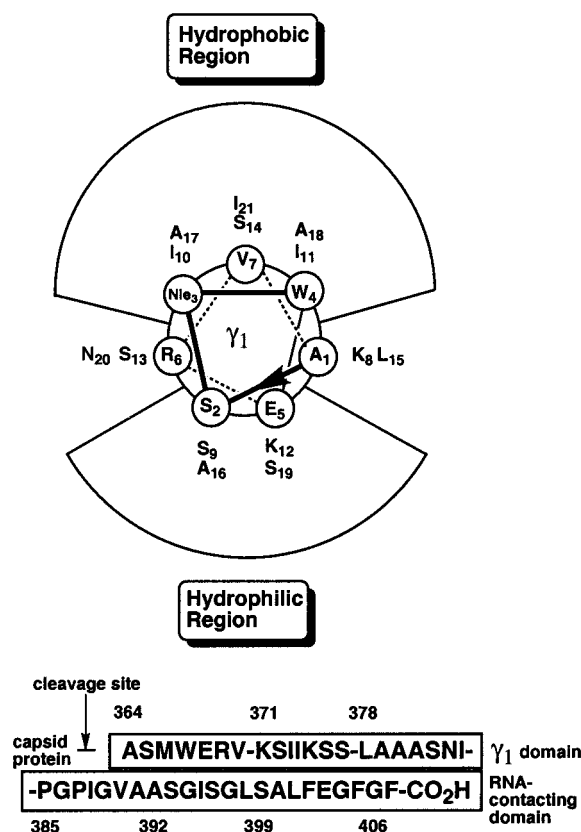
1-Palmitoyl-2-oleoyl-*sn*-glycero-3-phosphocholine (POPC), 1-palmitoyl-2-oleoyl-*sn*-glycero-3-phosphoglycerol (POPG), and 1,2-dipalmitoyl-*sn*-glycero-3-phosphoglycerol (DPPG) were purchased from Avanti Polar Lipids (Alabaster, AL). Methanol and chloroform were of HPLC and optima grade, respectively, and were obtained from Fisher Scientific. *Boc*-amino acids (Novabiochem, La Jolla, CA) were used as obtained, as

Received for publication 25 May 1999 and in final form 2 November 1999.

Address reprint requests to Dr. Reza Ghadiri, Departments of Chemistry and Molecular Biology, Skaggs Institute for Chemical Biology, The Scripps Research Institute, 10550 N. Torrey Pines Road, La Jolla, CA 92037. Tel.: 858-784-2743; Fax: 858-784-2798; E-mail: [ghadiri@scripps.edu](mailto:ghadiri@scripps.edu).

© 2000 by the Biophysical Society

0006-3495/00/02/839/07 \$2.00



Scheme 1 Helical wheel representation of  $\gamma_1$ . The numbered sequence of the entire  $\gamma$ -peptide is shown below, with cleavage site indicated with an arrow and helical and RNA contacting portions indicated in boxed regions.

was 2-(H-benzotriazole-1-yl)-1,1,3,3-tetramethyluronium hexafluorophosphate (HBTU) (Quantum Biotechnologies, Montreal, Canada). All lipids and solvents were used as purchased without further purification.

## Peptide synthesis

Manual *Boc* solid phase peptide synthesis was carried out according to the in situ neutralization protocol of Kent (Schnolzer et al., 1992) with HBTU activation on methylbenzhydrylamine (MBHA) resin (0.56 mEq/g loading). Formyl protection on tryptophan was removed before resin cleavage by treatment of the peptide with 10% hydrazine monohydrate in DMF at 0°C for 8 h. Peptides were cleaved from resin using standard HF procedures (10 ml 9:1 HF/anisole per gram of peptide resin; 2 h at 0°C) and eluted from the resin with TFA after washing with ethyl ether. The resulting free peptide solution was lyophilized, redissolved in acidic water/acetonitrile, and purified by reverse-phase HPLC on a Vydac C<sub>18</sub> column using a CH<sub>3</sub>CN/H<sub>2</sub>O/TFA gradient. The isosteric substitution of Met→Nle was made to obviate problems with thioether oxidation, and thus all measurements are done with  $\gamma_1$  peptide, which bears this substitution.

## Liposome preparation

Lipids were used as purchased to prepare films by drying the lipid dissolved in chloroform under a stream of nitrogen while heating, followed by several hours under vacuum. Multilamellar vesicles were prepared by swelling the lipid film in 100 mM acetate buffer at pH 5.0–5.5 while incubating at 65°C for 30 min with periodic vortexing for 30 s. The

resulting multilamellar vesicles were then sized at 65°C by extrusion through stacked polycarbonate membranes with pore diameters of ~200 nm using a miniextruder (LiposoFast, Avestin) to obtain LUVs. Lipid concentration was determined after extrusion by lyophilization of a known volume of the LUV suspension and analysis of the resulting powder by <sup>1</sup>H-NMR in CDCl<sub>3</sub>, using dioxane or benzene as an internal standard for peak integration. An acquisition delay of 15 s was used to ensure integration accuracy. Peptide concentration was determined by UV spectroscopy assuming an extinction coefficient of 5570 cm<sup>-1</sup> M<sup>-1</sup> at 280 nm.

## Fluorescence measurements

All fluorescence emission measurements were performed on an Aminco/Bowman luminescence spectrometer equipped with a water-jacketed sample chamber thermostatted at 25°C. Each spectrum was background corrected (buffer and vesicle light-scattering). Tryptophan fluorescence was monitored from 300 to 450 nm with excitation at 280 nm and 4-nm bandpass through a 300-nm low-pass filter (Hoya Optics).

## CD spectroscopy

CD spectra were obtained using an Aviv 62DS (Lakewood, NJ) spectrograph. Samples were scanned in a 0.2 cm CD-cell from 260 to 190 nm with 0.1 nm resolution and 1 nm bandwidth in a water-jacketed sample chamber thermostatted at 25°C. Ellipticity is reported as mean residue ellipticity in deg<sup>-1</sup> cm<sup>2</sup>/dmol. DPPC-LUVs were added to a 20–50  $\mu$ M peptide solution for CD measurement (lipid to peptide ratio 30:1, 100 mM acetate buffer, pH 5.0); spectra were background-corrected for light scattering and buffer absorption. Reported CD spectra are the average of six wavelength scans. Spectra were deconvoluted to determine secondary structure content using neural network-based deconvolution software (Boehm et al., 1992; Dalmas et al., 1994).

## Isothermal titration calorimetry

All calorimetric experiments were performed on a Microcal (Northampton, ME) MCS-ITC titration calorimeter in 100 mM acetate buffer at pH 4.8. Peptide solutions at concentrations ranging from 0.129 mM to 0.150 mM were injected in 10- $\mu$ l increments into the Hastaloy titration cell containing either the same buffer or a 13–20-mM suspension of LUVs. For each run the series of 10- $\mu$ l injections was preceded by a 1- $\mu$ l injection to equilibrate the injection apparatus. At this pH, the peptide dilution heat was negligible. At neutral pH, the dilution profile of  $\gamma_1$  suggested an aggregated state that was not seen at pH 5.5. Because high lipid concentrations can alter the pH of buffered solutions, the peptide titrant was pH matched to the LUV preparation for each titration run. The resulting cell power versus time traces were baseline-corrected and each peak was integrated to obtain heat evolved per injection.

## Analysis of $\gamma_1$ binding to fluid phase vesicles

As previously reported (Janshoff et al., 1999), incorporation of  $\gamma_1$  into lipid bilayers proceeds with induction of  $\alpha$ -helicity from random coil conformations and blue-shifting of tryptophan fluorescence. Changes in fluorescence, ellipticity, and heat were monitored during the course of peptide-lipid titrations in order to elucidate the thermodynamic behavior of the  $\gamma_1$ -lipid interaction. As bilayer fluidity contradicts conventional notions of binding in which the bound peptide has well-defined contacts, we have applied a surface partitioning model (Schwarz et al., 1986; Schwarz, 1989; Seelig, 1997) which is more appropriate for this system. Fluorescence and CD titrations in varying concentration regimes allowed the calculation of surface partition constants ( $K_p$ ) for  $\gamma_1$  into both POPC and POPG, while calorimetry directly revealed the enthalpy of peptide partitioning from

aqueous to lipid phases. Surface partition constants were extracted from lipid to peptide titration experiments by fitting the data to the following equation:

$$\Delta Q = \Delta Q_{\max} \frac{Kc_L}{1 + Kc_L} \quad (1)$$

where  $\Delta Q$  is the change in the observable (e.g., fluorescence intensity, ellipticity, or heat) at a given time, and  $\Delta Q_{\max}$  is the maximum change of the observable at infinite lipid/peptide ratios, obtained by fitting the raw data. The partition constant of  $\gamma_1$  into lipid is represented by  $K$ , and  $c_L$  is the concentration of accessible lipid (60% of the total lipid concentration, representing the outer leaflet of the membrane bilayer) at any given time. Assuming that  $\Delta Q/\Delta Q_{\max}$  is equivalent to  $c_B/c_P$ , where  $c_P$  is the total peptide concentration, then Eq. 1 derives directly from the definition of the surface partition constant  $K$ :

$$\frac{c_B/c_L}{c_f} = K \quad (2)$$

where  $c_B$ ,  $c_L$ , and  $c_f$  represent the concentration of lipid-associated (bound) peptide, total lipid concentration, and concentration of free peptide, respectively.

## RESULTS

### Fluorescence spectroscopy

Integration of  $\gamma_1$  into fluid phospholipid vesicles occurs with a significant blue-shift in the fluorescence emission maximum of tryptophan 4 as a result of the transition from a high dielectric environment (water) to a low one (lipid). While the fluorescence spectrum of peptide in aqueous buffer displays an emission maximum at 348 nm, the step-wise addition of POPC LUVs leads to a substantial 18-nm blue-shift at a high lipid/peptide ratio of 200:1. This fluorescence blue-shift was monitored as POPC liposomes were titrated into a peptide solution, providing a titration curve (Fig. 1) that fits well to Eq. 1. Plotting the degree of binding,  $c_B/c_L$  (symbolized as  $r$ ) against  $c_f$  (Fig. 1 B) reveals the expected linear relationship with slope of  $K = (7420 \pm 700) \text{ M}^{-1}$ .

Titration at high lipid/peptide mole ratios enjoy an additional advantage in that membrane bound peptide concentrations never become large enough to significantly alter the surface potential of the electrically neutral POPC. Indeed, at elevated  $r$  values the amount of bound, positively charged peptide alters the surface potential enough to affect binding, as one begins to observe charge-charge repulsion between bound and solution peptide reflected in the shape of the partition isotherm. Similarly, isotherm shape deviates from Eq. 1 when  $\gamma_1$  titrations are performed with negatively charged POPG LUVs. These deviations from the model result from both attractive and repulsive electrostatic forces between peptide and surface that create a different peptide concentration at the membrane surface than in bulk solution. Such electrostatic effects can be accounted for in the system model using a simple Gouy-Chapman formalism

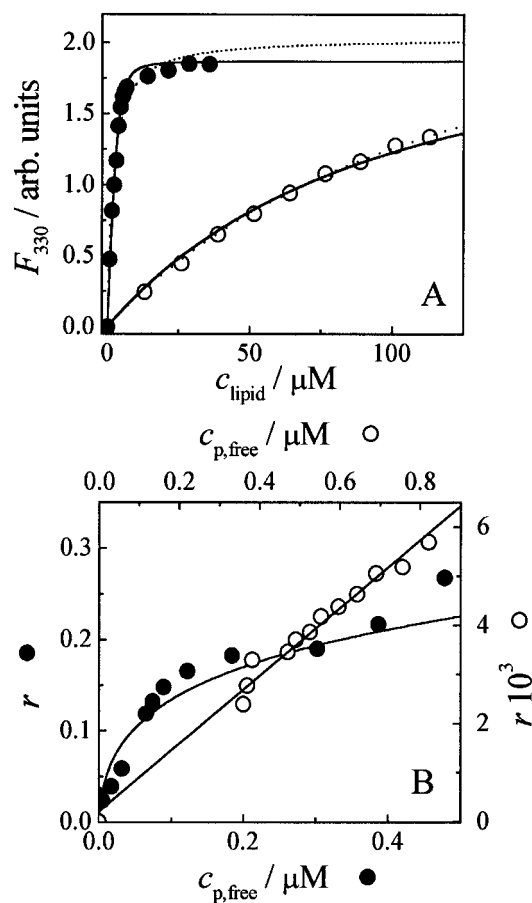


FIGURE 1 (A) The dependence of fluorescence intensity  $F$  at 330 nm of  $\gamma_1$ 's Trp-4 on lipid concentration in solution is displayed. POPC LUVs ( $\circ$ ) and POPG LUVs ( $\bullet$ ) were added to a  $\gamma_1$  solution ( $0.9 \mu\text{M}$ ) in 100 mM HAc, pH 5.0, and the fluorescence intensity was measured between 300 and 450 nm and background corrected. The dotted lines are Langmuir-type fits according to Eq. 2 neglecting the electrostatic interaction:  $K_{\text{POPC}} = (7420 \pm 700) \text{ M}^{-1}$ ,  $K_{\text{POPG}} = (52,000 \pm 6000) \text{ M}^{-1}$ . The solid lines are simulations according to Eq. 2 that account for surface-peptide electrostatics. Shown are curve simulations that assume a net peptide charge of  $z_p = 1.3$ ,  $K_{\text{POPC}} = 7420 \text{ M}^{-1}$ , and  $K_{\text{POPG}} = 12,000 \text{ M}^{-1}$ . (B)  $r$  vs.  $c_{\text{p, free}}$  presentation of the same data presented in (A).

(McLaughlin, 1989), (Eq. 3):

$$\Delta Q = \Delta Q_{\max} \left[ \frac{Kc_L}{\exp\left(\frac{z_p \Psi F}{RT}\right) + Kc_L} \right] \quad (3)$$

where  $z_p$  is the charge on the peptide,  $\Psi$ , is the membrane surface potential,  $F$  is Faraday's constant,  $R$  is the universal gas constant,  $T$  is temperature (Kelvin) and the remaining parameters are as described in Eq. 1. Note that at a surface potential of zero Eq. 3 simplifies to Eq. 1. A simulation using Eq. 3 with  $z_p = 1.3$  (vide infra) and  $K = 7420 \text{ M}^{-1}$  (corresponding to a partitioning energy of  $-7.5 \text{ kcal/mol}$  (Table 1.)) fits the POPC- $\gamma_1$  experimental data (Fig. 1 A) very well, demonstrating the validity of this method.

**TABLE 1** Thermodynamic parameters of  $\gamma_1$ -membrane partitioning

	POPC bilayer	POPG bilayer
$K$	$(5000 \pm 1000) \text{ M}^{-1}$	$12,000 \text{ M}^{-1}$
$\Delta G$	$(-7.5 \pm 0.1) \text{ kcal/mol}$	$-8.0 \text{ kcal/mol}$
$\Delta H$	$(-4.1 \pm 0.2) \text{ kcal/mol}$	$10.2 \text{ kcal/mol}$
$\Delta S$	$11.4 \text{ cal/mol} \cdot \text{deg}$	$61.1 \text{ cal/mol} \cdot \text{deg}$

Thermodynamic data of the binding of  $\gamma_1$  peptide to POPC and POPG LUVs. Enthalpy ( $\Delta H$ ) is obtained from ITC experiments titrating  $\gamma_1$  peptide to an excess of liposomes. Binding constants are mean values of five measurements combining CD and fluorescence experiments. The free energy of partitioning ( $\Delta G$ ) is calculated from  $\Delta G = -RT \ln(55.5K)$ .

Titration of  $\gamma_1$  peptide with negatively charged POPG vesicles reveals a much earlier saturation point of the tryptophan blue-shift (lipid/peptide ratio of 25:1) than with the zwitterionic POPC vesicles (lipid/peptide ratio of 200:1). As expected, favorable electrostatics between the negative membrane surface and the positively charged (basic)  $\gamma_1$  greatly enhance the peptide-to-lipid association equilibrium. When experimental partitioning curves (Fig. 1) using the fluorescence method were matched to simulations of Eq. 3, the highest accordance was found with a net peptide charge  $z_p$  of 1.3 (as seen in the POPC titration), and a POPG surface partition constant  $K = 12,000 \text{ M}^{-1}$  corresponding to a free energy of partitioning of  $-8.0 \text{ kcal/mol}$  (Table 1).

### CD spectroscopy

In buffer, the  $\gamma_1$  peptide exhibits a predominately (40%) random coil secondary structure (Fig. 2). However, titration with LUVs consisting of partially unsaturated phospholipids like POPC or POPG at room temperature results in a considerable increase (75%) in  $\alpha$ -helicity (Fig. 2, POPG titration). Examination of the lipid-dependent CD spectra of  $\gamma_1$  (Fig. 2) reveals an isodichroic point at 204 nm, indicating a two-state transition between random coil and  $\alpha$ -helix conformations. Addition of gel phase DPPG vesicles ( $T_m = 41^\circ\text{C}$ ) also results in an increase in helicity (>50%  $\alpha$ -helix content), whereas titration of DPPC liposomes below  $T_m$  does not significantly affect the secondary structure of the peptide (20%→26%). However, incubating the peptide-DPPC system above its phase transition temperature ( $T_m = 41^\circ\text{C}$ ) at  $55^\circ\text{C}$  for 30 min results in a substantial increase in  $\alpha$ -helix content (66%). Therefore, folding of the  $\gamma_1$  peptide in the presence of liposomes is induced by interaction of the peptide with the hydrophobic interior of the liposomes and by attractive electrostatic forces at the interface of the negatively charged PG headgroups.

Partitioning curves obtained from CD titrations yielded a partition constant  $K$  of  $17,000 \text{ M}^{-1}$  with a net peptide charge  $z_p$  of 1.3 (Fig. 2). Though the consensus net charge of 1.3 obtained by fitting these partitioning curves falls short of the number expected (3) from the amino acid composition of  $\gamma_1$  (Scheme 1), this may be a result of a number of

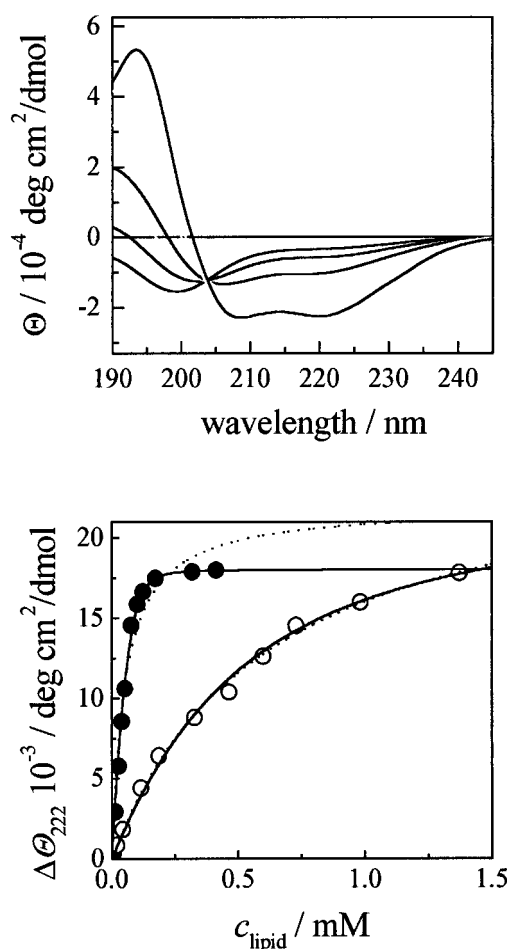


**FIGURE 2** *Top:* circular dichroism spectra of a typical titration of  $\gamma_1$  peptide with different amounts of POPG LUVs. Ellipticity at 222 nm decreases with increasing lipid concentration, from 0 to 1.5 mM. *Bottom:* POPC LUVs (○) and POPG LUVs (●) were added to a  $\gamma_1$  solution (20–50  $\mu\text{M}$ ) in 200 mM HAc, pH 5.0 and the circular dichroism was measured between 260 and 190 nm and background-corrected. The dotted lines are Langmuir-type fits according to Eq. 2 neglecting the electrostatic interaction:  $K_{\text{POPC}} = (1600 \pm 200) \text{ M}^{-1}$ ,  $K_{\text{POPG}} = (19,000 \pm 3000) \text{ M}^{-1}$ . The solid lines are simulations according to Eq. 2 taking the electrostatic interaction into account. Shown are best accordance simulations assuming a net peptide charge of  $z_p = 1.3$ ,  $K_{\text{POPC}} = 4000 \text{ M}^{-1}$ , and  $K_{\text{POPG}} = 17,000 \text{ M}^{-1}$ .

reasons, such as  $\text{pK}_A$  shifts at the surface, charge shielding, or the presence of discrete charges at the surface (Beschiachvili and Baeuerle, 1991) instead of the smeared charge distribution assumed in Gouy-Chapman theory (Stankowski, 1991). Interestingly, unlike the situation observed with melittin (Kuchinka and Seelig, 1989; Schwarz and Beschiachvili, 1989), one observes a two- to threefold superiority in the association constant of  $\gamma_1$  with POPG over POPC, even after correcting for electrostatic effects. The larger POPG partitioning constant most likely derives from the lower density of lipid packing resulting from charge repulsion between headgroups. This, in turn, would facili-



tate peptide integration into POPG bilayers over POPC, resulting in tighter binding. Though electrostatic interactions in POPG membranes enhance partitioning, these association constants clearly reveal that  $\gamma_1$  partitions spontaneously into both neutral and charged lipid phases.

### Isothermal titration calorimetry

Ultrasensitive titration calorimetry was used to directly determine the heat of peptide-lipid binding. In this experiment, heat flow was monitored while a dilute peptide solution in acidic buffer was titrated into a suspension of POPC or POPG LUVs (Fig. 5), revealing the heat of  $\gamma_1$  binding to POPC and POPG membranes to be  $-4$  kcal/mol and  $+10$  kcal/mol, respectively (Fig. 3, Table 1). Notably, the binding enthalpy changes from exothermic to endothermic when negatively charged POPG liposomes are used instead of

zwitterionic POPC vesicles. Endothermic binding has been observed for other peptide-lipid interactions (Seelig, 1997; Montich et al., 1993), in which peptide insertion into the lipid matrix disrupts hydrocarbon packing with an entropically favorable release of water from the peptide but without commensurate peptide-lipid van der Waals interactions. However, peptide binding to neutral POPC is enthalpically favorable, and since the hydrocarbon matrix of this lipid is similar to that of POPG, it appears that the endothermic binding to the negatively charged POPG is largely a head-group effect. Indeed, treatment of gel phase DPPG with peptide results in an even stronger endothermic heat of  $+20$  kcal/mol (data not shown). As a result of the more tightly packed saturated lipids in a DPPG bilayer, the peptide is unable to insert into the hydrocarbon environment, and thus the heat of peptide-headgroup interaction is isolated. Additionally, titration of nodaviral peptide with gel phase DPPC liposomes revealed a negligible interaction enthalpy (data not shown). Therefore, the DPPG titration provides a rough approximation of the relative contributions of headgroup electrostatics ( $+20$  kcal/mol, from DPPG titration) and hydrophobic contacts ( $-4$  kcal/mol, from POPC titration) to the heat of peptide partitioning into POPG ( $+10$  kcal/mol). The endothermicity of headgroup binding may derive from disruption of hydration shells surrounding the negatively charged phosphoglycerol headgroups, though this is as yet unclear. While the exothermic  $\gamma_1$  binding to POPC is similar to published calorimetric measurements of interactions between membrane active peptides and electrically neutral membranes, to our knowledge, the change from exothermic to endothermic heats upon binding negatively charged membranes has not been previously reported.

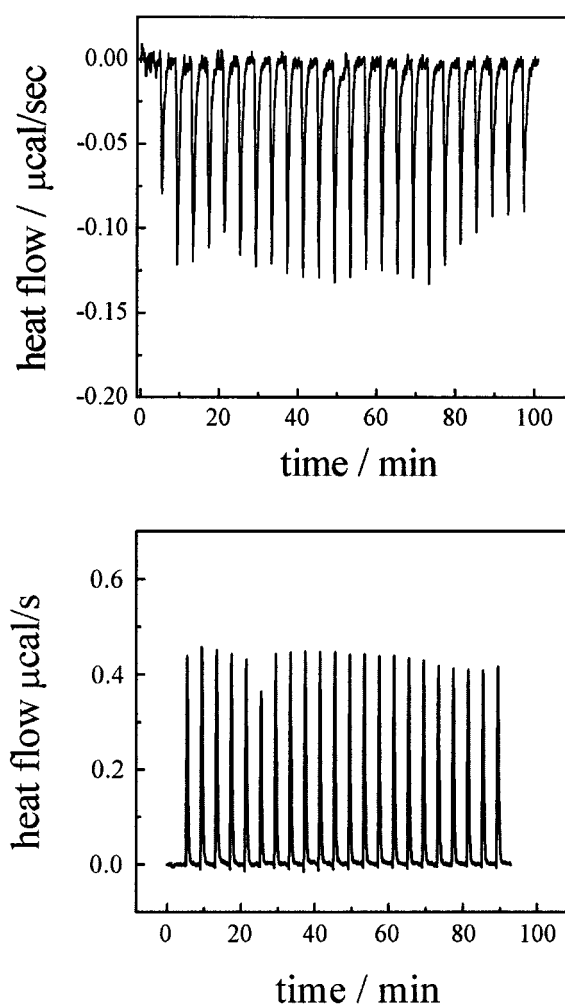


FIGURE 3 Titration calorimetric traces describing the change in titration cell power versus time. An  $0.129$  mM solution of  $\gamma_1$  was injected in  $10\ \mu\text{l}$  increments into the titration cell, which contained either a  $20.31$  mM suspension of POPC LUVs (top) or a  $13.79$  mM suspension of POPG LUVs (bottom).

### DISCUSSION

Biophysical studies have shown  $\gamma_1$  to be an extremely membrane-active species that binds avidly to fluid phase lipid bilayers and increases transmembrane permeability. To gain further insight into the mechanisms by which this occurs in liposomal membranes, we obtained a full thermodynamic description of  $\gamma_1$  binding to LUVs and analyzed the binding behavior in the context of the effect of  $\gamma_1$  on membrane function. We have found that  $\gamma_1$  displays similar activity and thermodynamic profile to known membrane active peptides such as melittin ( $\Delta G_{\text{partition}} = -8.7$  kcal/mol) (Schwarz and Beschiaschvili, 1989; Stankowski et al., 1991; Kuchinka and Seelig, 1989; Beschiaschvili and Seelig, 1990a) and alamethicin ( $\Delta G_{\text{partition}} = -6.5$  kcal/mol) (Archer et al., 1991; Rizzo et al., 1987; Schwarz et al., 1986). Lipid titration experiments tracing the thermodynamic profile of peptide-lipid association have testified to the high capacity of the viral peptide segment  $\gamma_1$  to partition into lipid bilayers. Our CD titration experiments have demonstrated the induction of helicity in the  $\gamma_1$  peptide upon addition of liposomes, thus defining the secondary structure

of the lipid-bound peptide. Since the transfer of hydrophobic protein from water to a low dielectric environment (such as a lipid bilayer) results in a  $-15$  to  $-20$  calorie free energy change per  $\text{\AA}^2$  of buried protein surface (Janin and Chothia, 1978), the free energy of peptide-lipid partitioning indicates that 50–70% of the helical surface of  $\gamma_1$  contacts the lipid matrix in both POPC and POPG liposome-peptide associates. (The random coil to  $\alpha$ -helix folding transition that accompanies membrane insertion contributes a negligible  $0.4$  kcal/mol (Park et al., 1993).) These values closely complement the fluorescence quenching data and ATR-IR analysis of  $\gamma_1$ -lipid complexes, which place this helical region of the FHV cleavage sequence  $\sim 1$  nm from the bilayer midplane, with its helical axis roughly perpendicular to the membrane surface normal (Bong et al., 1999). Thus, these measurements concur that only half of the peptide surface packs against the lipid matrix while the other half remains solvent-exposed, as expected for an amphiphilic helix (Fig. 4).

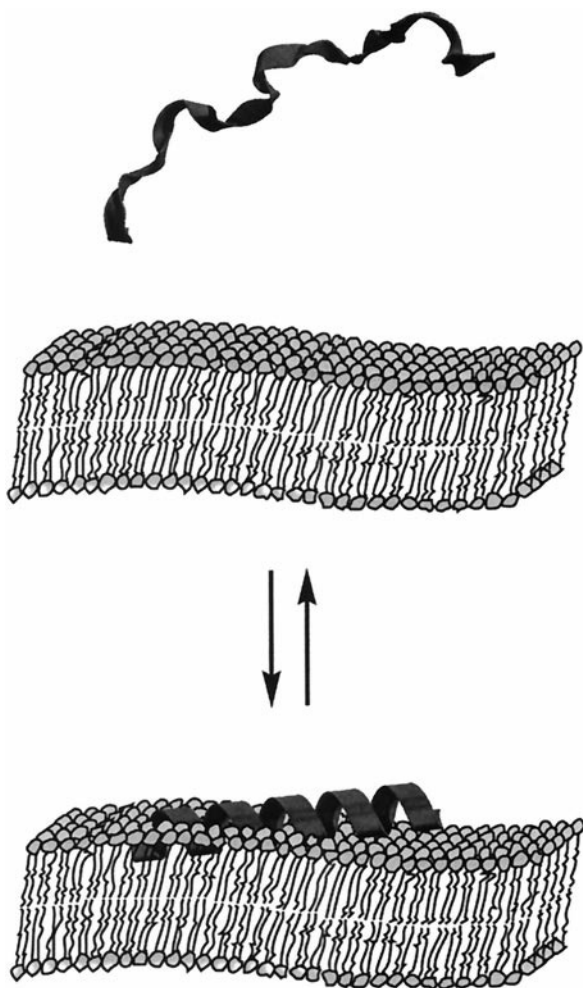


FIGURE 4 A schematic depiction of the formation of the peptide-lipid complex, based on our biophysical data. The random coil  $\gamma_1$  peptide is shown in solution as a gray ribbon that becomes helical upon incorporation into a lipid bilayer.

Furthermore, membrane electrostatic complementarity that would be present in natural systems was shown to dramatically increase bilayer partitioning of  $\gamma_1$  peptide. Further, POPG association with  $\gamma_1$  is completely entropy-driven, with a positive enthalpy of interaction while peptide partitioning into POPC is predominately enthalpy-driven (Table 1). It is likely that the favorable electrostatics between headgroup and peptide in the POPG system serve to decrease the off-rate of  $\gamma_1$  from the membrane surface, thus resulting in an earlier lipid-peptide saturation point and decreased penetration depth into the bilayer. Assuming a viral host membrane with a typical net negative charge, this partitioning profile suggests that externalization of the  $\gamma_1$  region from the interior of FHV during the course of infection would result in rapid localization of the amphipathic peptide into the headgroup region of the host membrane. The efficient membrane partitioning capabilities of  $\gamma_1$  reported here are consistent with the proposed membrane-broaching function of the  $\gamma$  cleavage peptide of FHV, validating further in vivo investigation of this hypothesis.

## APPENDIX

### Model for binding of $\gamma$ -peptide to liposomes

Previous studies have shown that the assumption of a surface partition equilibrium of the peptide between the lipid and water phase is suitable to describe the binding of small neutral peptides to neutral liposomes such as POPC (Schwarz and Beschiaschvili, 1989). A simple Gouy-Chapman approach was used to account for electrostatic interactions of either repulsive nature in the case of adsorption of the positively charged peptide on POPC or attractive nature when POPG was used. The influence of the surface potential over the membrane is treated by means of the Gouy-Chapman theory yielding:

$$\Theta = \frac{Kc_L}{\exp\left(\frac{z_p \Psi F}{RT}\right) + Kc_L} \quad (\text{A1})$$

in which the surface potential can be obtained from:

$$\sigma^2 = 2\epsilon_0\epsilon_r kT \left( \sum_i c_{0,i} \exp\left(\frac{-z_i F \Psi}{RT}\right) - \sum_i c_{i,0} \right), \quad (\text{A2})$$

where  $\sigma$  is the surface charge density of the liposome and  $c_{i,0}$  is the concentration of the dissociated electrolyte solution. However, two corrections for calculation of  $\sigma$  in the case of peptide binding to POPG are necessary. First the binding of sodium ions to the PG headgroups in a Langmuir type adsorption isotherm have to be considered and second the expansion of the bilayer structure upon integration of the peptide in the lipid matrix. Both corrections (Beschiaschvili and Seelig, 1990b) result in a decrease of the initial charge density of the POPG bilayer:

$$\sigma = \frac{e_0}{A_{\text{lipid}}} \left( \frac{\frac{c_{p,\text{bound}}}{c_L} z_p - 1}{\left(1 + \frac{A_p c_{p,\text{bound}}}{A_{\text{lipid}} c_L}\right) \left(1 + K_{\text{Na}} c_{\text{Na}} \exp\left(\frac{\Psi F}{RT}\right)\right)} \right), \quad (\text{A3})$$

where  $A_{\text{lipid}}$  is the area of the PG headgroup ( $0.68 \text{ nm}^2$ ),  $A_p$  is the area of the  $\gamma_1$  peptide ( $5.1 \text{ nm}^2$ ; assuming an  $\alpha$ -helical  $\gamma_1$  peptide lying flat on the bilayer),  $e_0$  is the elementary charge ( $1.602 \cdot 10^{-19} \text{ C}$ ), and  $K_{\text{Na}}$  is the binding constant of sodium with a concentration  $c_{\text{Na}}$  to PG ( $0.6 \text{ M}^{-1}$ ). These corrections were used to simulate the binding curves of  $\gamma_1$  to POPG and POPC liposomes.

We gratefully acknowledge Professor J. W. Kelly's assistance with isothermal titration calorimetry.

## REFERENCES

- Archer, S. J., J. F. Ellena, and D. S. Cafiso. 1991. Dynamics and aggregation of the peptide ion channel alamethicin. Measurements using spin-labeled peptides. *Biophys. J.* 60:389–398.
- Beschiaschvili, G., and H. D. Baeuerle. 1991. Effective charge of melittin upon interaction with POPC vesicles. *Biochim. Biophys. Acta.* 1068: 195–200.
- Beschiaschvili, G., and J. Seelig. 1990a. Melittin binding to mixed phosphatidylglycerol/phosphatidylcholine membranes. *Biochemistry.* 29:52–58.
- Beschiaschvili, G., and J. Seelig. 1990b. Peptide binding to lipid bilayers. Binding isotherms and zeta-potential of a cyclic somatostatin analog. *Biochemistry.* 29:10995–11000.
- Boehm, G., R. Muhr, and R. Jaenicke. 1992. Quantitative analysis of protein far UV circular dichroism spectra by neural networks. *Protein Eng.* 5:191–195.
- Bong, D. T., C. Steinem, A. Janshoff, J. E. Johnson, and M. R. Ghadiri. 1999. A highly membrane active peptide in Flock House Virus: implications for the mechanism of nodavirus infection. *Chemistry and Biology.* 6:473–481.
- Cheng, R. H., V. S. Reddy, N. H. Olson, A. J. Fisher, T. S. Baker, and J. E. Johnson. 1994. Functional implications of quasi-equivalence in a T = 3 icosahedral animal virus established by cryo-electron microscopy and x-ray crystallography. *Structure (Lond.).* 2:271–282.
- Dalmas, B., G. J. Hunter, and W. H. Bannister. 1994. Prediction of protein secondary structure from circular dichroism spectra using artificial neural network techniques. *Biochem. Mol. Biol. Int.* 34:17–26.
- Fisher, A. J., and J. E. Johnson. 1993. Ordered duplex RNA controls capsid architecture in an icosahedral animal virus. *Nature (Lond.).* 361: 176–179.
- Hosur, M. V., T. Schmidt, R. C. Tucker, J. E. Johnson, T. M. Gallagher, B. H. Selling, and R. R. Rueckert. 1987. Structure of an insect virus at 3.0 Å resolution. *Proteins: Struct., Funct., Genet.* 2:167–176.
- Janin, J., and C. Chothia. 1978. Role of hydrophobicity in the binding of coenzymes. *Biochemistry.* 17:2943–2948.
- Janshoff, A., D. T. Bong, C. Steinem, J. E. Johnson, and M. R. Ghadiri. 1999. An animal virus-derived peptide switches membrane morphology: possible relevance to nodaviral transfection processes. *Biochemistry.* 38:5328–5336.
- Kuchinka, E., and J. Seelig. 1989. Interaction of melittin with phosphatidylcholine membranes. Binding isotherm and lipid head-group conformation. *Biochemistry.* 28:4216–4221.
- McLaughlin, S. 1989. The electrostatic properties of membranes. *Annu. Rev. Biophys. Biophys. Chem.* 18:113–136.
- Montich, G., S. Scarlata, S. McLaughlin, R. Lehrmann, and J. Seelig. 1993. Thermodynamic characterization of the association of small basic peptides with membranes containing acidic lipids. *Biochim. Biophys. Acta.* 1146:17–24.
- Munshi, S., L. Liljas, J. Cavarelli, W. Bomu, B. McKinney, V. Reddy, and J. E. Johnson. 1996. The 2.8 Å structure of a T = 4 animal virus and its implications for membrane translocation of RNA. *J. Mol. Biol.* 261: 1–10.
- Park, S.-H., W. Shaolongo, and E. Stellwagen. 1993. Residue helix parameters obtained from dichroic analysis of peptides of defined sequence. *Biochemistry.* 32:7048–7053.
- Rizzo, V., S. Stankowski, and G. Schwarz. 1987. Alamethicin incorporation in lipid bilayers: a thermodynamic study. *Biochemistry.* 26: 2751–2759.
- Schneemann, A., and D. Marshall. 1998. Specific encapsulation of nodavirus RNAs is mediated through the C terminus of capsid precursor protein alpha. *J. Virol.* 72:8738–8746.
- Schneemann, A., W. Zhong, T. M. Gallagher, and R. R. Rueckert. 1992. Maturation cleavage required for infectivity of a nodavirus. *J. Virol.* 66:6728–6734.
- Schnolzer, M., P. Alewood, A. Jones, D. Alewood, and S. B. H. Kent. 1992. In situ neutralization in Boc-chemistry solid phase peptide synthesis. Rapid high yield assembly of difficult sequences. *Int. J. Peptide Protein Res.* 40:180–193.
- Schwarz, G. 1989. Thermodynamics and kinetics of incorporation into a membrane. *Biochimie.* 71:1–9.
- Schwarz, G., and G. Beschiaschvili. 1989. Thermodynamic and kinetic studies on the association of melittin with a phospholipid bilayer. *Biochim. Biophys. Acta.* 979:82–90.
- Schwarz, G., S. Stankowski, and V. Rizzo. 1986. Thermodynamic analysis of incorporation and aggregation in a membrane: application to the pore-forming peptide alamethicin. *Biochim. Biophys. Acta.* 861: 141–151.
- Seelig, J. 1997. Titration calorimetry of lipid-peptide interactions. *Biochim. Biophys. Acta.* 1331:103–116.
- Stankowski, S. 1991. Surface charging by large multivalent molecules. Extending the standard Gouy-Chapman treatment. *Biophys. J.* 60: 341–351.
- Stankowski, S., M. Pawlak, E. Kaisheva, C. H. Robert, and G. Schwarz. 1991. A combined study of aggregation, membrane affinity and pore activity of natural and modified melittin. *Biochim. Biophys. Acta.* 1069: 77–86.
- Zlotnick, A., V. S. Reddy, R. Dasgupta, A. Schneemann, W. J. Ray, Jr., R. R. Rueckert, and J. E. Johnson. 1994. Capsid assembly in a family of animal viruses primes an autoproteolytic maturation that depends on a single aspartic acid residue. *J. Biol. Chem.* 269:13680–13684.